Article

Not peer-reviewed version

Global Profile of tRNA-Derived Small RNAs in Pathological Cardiac Hypertrophy Plasma and Identification of tRF-21-NB8PLML3E as a New Hypertrophy Suppressor

Jingyi Xu , Buyun Qian , Feng Wang * , Ying Huang , Xinxin Yan , Ping Li , Qian Zhang , Yuan Li , Kangyun Sun *

Posted Date: 24 April 2023

doi: 10.20944/preprints202304.0855.v1

Keywords: transfer RNA-derived small RNAs; pathological cardiac hypertrophy; small RNA sequencing; biomarkers

Article

Global Profile of tRNA-Derived Small RNAs in Pathological Cardiac Hypertrophy Plasma and Identification of tRF-21-NB8PLML3E as a New Hypertrophy Suppressor

Jingyi Xu [2,†], Buyun Qian [1,†], Feng Wang [3], Ying Huang [2], Xinxin Yan [3], Ping Li [2], Qian Zhang [3], Yuan Li [1,*] and Kangyun Sun [1,*]

[1] Department of Cardiology, The Affiliated Suzhou Hospital of Nanjing Medical University, Suzhou Municipal Hospital, Gusu School, Nanjing Medical University, Suzhou, Jiangsu 215008, PR China
[2] Department of Central Laboratory, The Affiliated Suzhou Hospital of Nanjing Medical University, Suzhou Municipal Hospital, Gusu School, Nanjing Medical University, Suzhou, Jiangsu 215008, PR China
[3] Department of Pharmacy, The Affiliated Suzhou Hospital of Nanjing Medical University, Suzhou Municipal Hospital, Gusu School, Nanjing Medical University, Suzhou, Jiangsu 215008, PR China
* Correspondence: author: Kangyun Sun, Email: sunkangyun@njmu.edu.cn; Yuan Li, Email: Liyuan1596215@163.com
† Jingyi Xu and Buyun Qian contributed equally to this work.

Abstract: Background: It remains unclear whether transfer RNA-derived small RNAs (tsRNAs) play a role in pathological cardiac hypertrophy (PCH). We aimed to clarify the expression profile of tsRNAs and disclose their relationship to the clinical phenotype of PCH and the putative role. **Methods:** Small RNA sequencing was performed in the plasma of PCH patients and healthy volunteers. In a larger sample size and angiotensin II (Ang II)-stimulated H9c2 cells, the data were validated by real-time qPCR. The atrial natriuretic peptide (ANP) and brain natriuretic peptide (BNP) were examined in Ang II-stimulated H9c2 cells. The role of tsRNAs in the pathogenesis of PCH was explored by bioinformatics analysis. **Results:** A total of 4185 differentially expressed tsRNAs were identified, of which 4 and 5 tsRNAs were observed to be significantly differentially upregulated and downregulated expressed. Of the 5 down-regulated tsRNAs, 4 of them were verified to be significantly down-regulated in the larger sample group, among which tRF-30-3JVIJMRPFQ5D, tRF-16-R29P4PE, tRF-21-NB8PLML3E, and tRF-21-SWRYVMMV0 had areas under the curve to diagnose concentric hypertrophy. The 4 down-regulated tsRNAs were negatively correlated with left ventricular posterior wall dimensions in PCH patients (r = -0.4227; r = -0.4517; r = -0.5567; r = -0.4223). The levels of ANP and BNP as well as cell size were decreased in Ang II-stimulated H9c2 cells with 21-NB8PLML3E mimic transfection. Bioinformatics analysis revealed that the target genes of tRF-21-NB8PLML3E were mainly enriched in the metabolic pathway and involved in the regulation of ribosomes. **Conclusion:** The plasma tsRNAs tRF-21-NB8PLML3E might be considered biomarkers in patients with PCH with early screening potential.

Keywords: transfer RNA-derived small RNAs; pathological cardiac hypertrophy; small RNA sequencing; biomarkers

Introduction

Cardiac hypertrophy is the physiological adaptive response of the heart to maintain cardiac function against cardiac physiological and pathological overloading which is mainly characterized by an increased cardiomyocyte size and heart mass [1]. However, sustained pathological stress will lead to pathological cardiac hypertrophy (PCH), which is mainly manifested by enlarging cardiomyocyte size, cardiac fibrosis, and cardiomyocyte death [1,2]. As the disease progresses, pathological hypertrophy changes from a reduction in ventricular chamber dimension with increased wall thickness to ventricular chamber dilatation in the later stages, leading to heart failure progressively (Figure 1) [3]. From this, a better understanding of the key molecules in PCH may allow early diagnosis and targeted therapy to be developed.

Preprints (www.preprints.org) | NOT PEER-REVIEWED | Posted: 24 April 2023 doi:10.20944/preprints202304.0855.v1

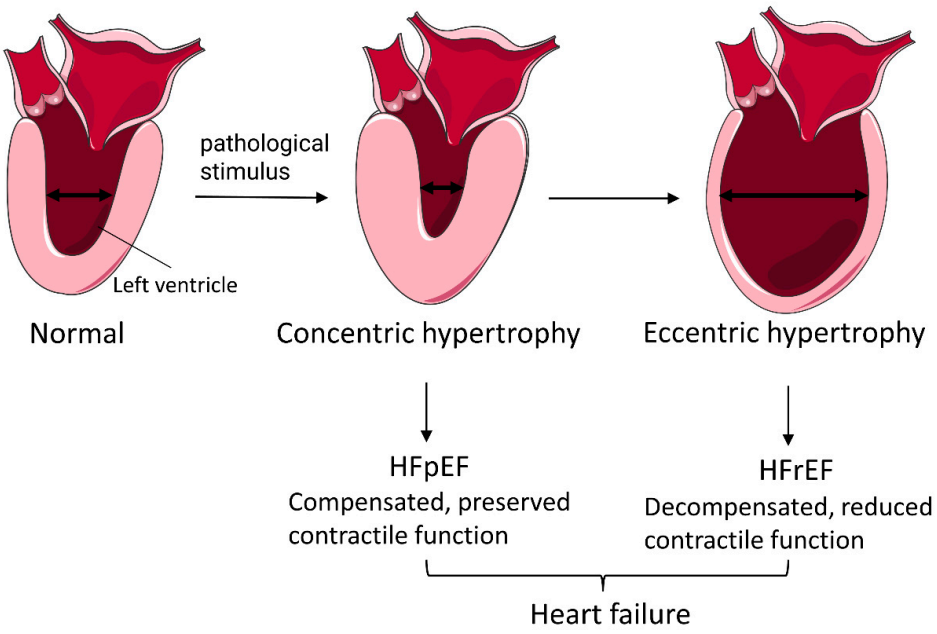

Figure 1. Overview of pathological cardiomyocyte hypertrophy. Pathological hypertrophy is initially identified by a reduction in ventricular chamber dimension with increased wall thickness (concentric hypertrophy), which results in HFpEF. As the disease progresses, pathological hypertrophy leads to ventricular chamber dilatation (eccentric hypertrophy) with impaired contractile function (maladaptive remodeling) which often results in HFrEF.

Studies have shown that noncoding RNAs (ncRNAs) play a significant role in PCH occurrence and development via regulation of cellular metabolism, translation regulation, and epigenetic modification [4–6]. Transfer RNAs (tRNAs) are one class of ncRNAs that deliver specific amino acids to ribosomes for protein synthesis [7]. It has been demonstrated that tRNAs can produce small ncRNAs called tRNA-derived small RNAs (tsRNAs) [8,9]. In terms of cleavage positions of tRNA precursors or mature transcripts, tsRNAs can be divided into two types, tRNA-related fragments (tRFs) and tRNA halves (tiRNAs) [10]. And based on their mapped positions, tsRNAs can be divided into five categories: tRF-1, tRF-3, tRF-5, internal tRF (i-tRF), and tiRNAs [9,11,12].

Many studies have demonstrated that tsRNAs are not simply random products of tRNA degradation, even though their specific biological functions have not been fully clarified [13,14]. They are involved in regulating various stages of gene expression, including transcription, translation, RNA processing and maturation, and related to key cellular processes such as self-renewal, differentiation, and proliferation [15–17]. For example, studies have demonstrated that tsRNAs can regulate mRNA stability in an RNA interference manner or regulate protein translation via competitive bidding to translation initiation complexes YBX1 [18,19]. However, a full understanding of tsRNA's potential role in PCH remains elusive.

This study was conducted to research the expression profiles of tsRNAs in PCH patients by RNA-sequencing, and the results were validated by real-time qPCR in larger sample-sized groups and Ang II-stimulated H9c2 cells. Afterward, the clinical diagnostic value of tsRNAs was analyzed and their possible biological function in the pathogenesis of PCH was initially explored.

Materials and Methods

Clinical Samples Collection

Between August 2021 and July 2022, 60 subjects aged 40-80 years (35 PCH patients and 25 healthy volunteers as controls) were enrolled in the study. PCH patients were from the Department of Cardiology of The Affiliated Suzhou Hospital of Nanjing Medical University, Gusu School, and

 doi:10.20944/preprints202304.0855.v1

the healthy volunteers were from Suzhou Physical Examination Center (Suzhou, China). The inclusion criteria of PCH patients were based on the "Chinese guidelines for the diagnosis and treatment of heart failure 2018", and patients with HFpEF and HFrEF were selected for inclusion. Patients with acute infection, myocardial infarction, severe primary disease, cerebral infarction, trauma, pregnancy, cancer, and drug or alcohol addiction were excluded from the study. During the same period, 25 healthy volunteers were recruited as the controls. The study was approved and supervised by the Ethics Committees of Affiliated Suzhou Hospital of Nanjing Medical University, Gusu School (K-2021-GSKY20210202).

Collection and Preparation of Plasma Samples

5 mL plasma was taken using EDTA vacuum anticoagulant blood vessels from the two groups just before treatment initiation. After centrifuging the blood samples at 1000 g for 10 minutes (4 °C), the plasma samples were collected and stored at −80 °C.

Library Preparation and tRFs & tiRNAs Sequencing

Plasma samples from 4 healthy volunteers were numbered A1 to A4 as controls and 4 PCH patients numbered B1 to B4. The total RNA was extracted with Trizol following the manufacturer's instructions. tsRNAs are heavily decorated with RNA modifications, which makes it difficult to construct small RNA sequence libraries. Before library preparation for total RNA samples, some treatments were performed: to ligate the 3′ adaptor, 3′ aminoacyl (charged) is deacylated to 3′-OH, and 3′-cP (2′, 3′-cyclic phosphate) is removed to generate 3′-OH. To ligate the 5′-adaptor, 5′-OH (hydroxyl group) is phosphorylated to form 5′-P. In addition, m1A and m3C are demethylated. To sequence RNA biotypes, sequencing libraries are size-selected using automated gel cutters. Agilent BioAnalyzer 2100 is used to qualify and quantify the libraries. tsRNAs sequencing was performed by Shanghai Kangcheng Technology co., Ltd.

Data Analysis of tsRNAs

Raw sequencing data generated from Illumina NextSeq 500 that passed the Illumina chastity filter was used for the following analysis. Aligned trimmed reads (trimmed 5′, 3′-adaptor bases) and unmapped reads separately using bowtie software. Their abundance was assessed by sequencing counts of tsRNAs and normalized as counts per million of total aligned reads (CPM). The differentially expressed tsRNAs were screened based on the count value with R package edgeR. Principal component analysis (PCA), Pie plots, Hierarchical clustering, Scatter plots and Volcano plots were calculated and graphed in an R or Perl environment.

Quantitative Real-Time PCR Validation

Real-time qPCR was used to validate the expression changes detected by RNA-sequencing of tsRNAs in a larger sample size and in Ang II-stimulated H9c2 cells. There are four up-regulated tsRNAs including tRF-19-8FFDXXE5, tRF-19-SWRYVMH0, tRF-16-Q622EVE, and tRF-26-YONONU3INDD, and five down-regulated tsRNAs including tRF-21-NB8PLML3E, tRF-18-F9LKXN05, tRF-21-SWRYVMMV0, tRF-16-R29P4PE, and tRF-30-3JVIJMRPFQ5D. We validated the down-regulated 5 tsRNAs. cel-miR-39-3p, a miRNA of C. elegans, was artificially added to plasma as external control, and U6 serves as an internal reference for the cell model. Total RNA was extracted from plasma with TRIzol Reagent (Thermo Fisher Scientific, Inc.). Then, the RNA was reverse-transcribed into cDNA and quantified by qPCR using PrimeScript™ RT Master Mix and TB Green® Premix Ex Taq™ II (Takara, Inc.) according to the manufacturer's protocols. The primers used in this experiment were shown in Table S1. PCR was performed in 20 μL reaction volume, including 10 μL 2× Real-time PCR Master Mix, 0.8 μL tRFs & tiRNA specific Primer set (10 μM), 2 μL cDNA, and 7.2 μL RNase free H_2O. The reaction was performed at 95 °C for 30 s, followed by 40 amplification cycles at 95 °C for 5 s, and 60°C for 30 s. The relative tsRNAs expression levels were calculated using the $2^{-\Delta\Delta Ct}$ method and were normalized to cel-miR-39-3p and U6, respectively.

 doi:10.20944/preprints202304.0855.v1

Cell Culture and Treatment

The rat H9c2 cell line was obtained from Fuheng BioLogy and cultured in DMEM medium supplemented with 10% fetal bovine serum, 100 IU/mL penicillin, and 100 μg/mL streptomycin and kept in an incubator containing 5% CO_2 at 37°C in a humidified atmosphere. After H9c2 cells were grown to 70% confluence, they were treated with 2 mM Ang II for 48 h. Finally, the cultured cells were harvested for the measurement of tRF-30-3JVIJMRPFQ5D, tRF-16-R29P4PE, tRF-21-NB8PLML3E, and tRF-21-SWRYVMMV0 mRNA expressions.

After the cells were stimulated with Ang II for 24 h, tRF-21-NB8PLML3E mimic or inhibitor (GenePharma, Inc.) were transfected for another 24 h, respectively. After that, the atrial natriuretic peptide (ANP) and brain natriuretic peptide (BNP) in the cell supernatant were detected according to the ELISA assay kit (Sinobestbio, Inc.) instructions.

Immunofluorescence

Immunofluorescence staining was used to observe tRF-21-NB8PLML3E mimic or inhibitor (GenePharma, Inc.) treated Ang II-stimulated H9c2 cells. The cells were fixed with 4% paraformaldehyde for 30 min, then incubated with 0.1% Triton X-100 for 30 min and finally blocked with 1% BSA for 1 h at room temperature. The phalloidin was placed on the glass slide and incubated for 20 min. DAPI was used to stain the nucleus. The confocal microscope was used to photograph the cells.

Bioinformatic Analysis

To analyze the possible biological functions of differentially expressed tsRNAs, the target genes of the tsRNAs were predicted using miRanda and TargetScan, and the GeneOntology (GO) project and the KEGG database were performed to analyze the biological functions of predicted target genes.

Statistical Analysis

The results were reported as the mean ± standard deviation (SD). Student's t-test was used to analyze two-group comparisons of quantitative data, and the $\chi 2$ test was performed for analyzing two-group comparisons of non-quantitative data. The clinical diagnostic value of candidate tsRNAs was evaluated by receiver operating characteristic (ROC) curve analysis, and the linear correlation in different groups was determined by Spearman analysis. P values <0.05 were considered significant. All the statistical analyses were performed using SPSS 19.0 (SPSS, Chicago, USA) and GraphPad Prism 8 (GraphPad, CA, USA).

Results

Characteristics of PCH Patients and Healthy Subjects

A total of 35 PCH patients and 25 healthy volunteers were enrolled in the experiment, and their baseline characteristics were shown in Table S2. The data showed that the majority of PCH patients were male. 37.1429% of PCH patients had diabetes mellitus, and 80% had hypertension, which significantly increased compared with the control group.

We divided 35 patients with PCH into 2 groups according to echocardiography, including 16 cases of concentric hypertrophy and 19 cases of eccentric hypertrophy. The cardiac structure and function of the two types of patients are shown in Table 1. According to the results of echocardiography, the left ventricular end-diastolic diameter (LVEDD), left ventricular end-systolic diameter (LVESD), and right ventricular diameter (RV) in patients with concentric hypertrophy are significantly lower than those in patients with eccentric hypertrophy. While the thickness of the interventricular septum (IVS), left ventricular posterior wall dimensions (LVPWd), and left ventricular ejection fraction (LVEF) were significantly higher than those of the patients with eccentric hypertrophy.

Preprints (www.preprints.org) | NOT PEER-REVIEWED | Posted: 24 April 2023 doi:10.20944/preprints202304.0855.v1

Table 1. Cardiac structure and function in different stages of PCH.

characteristics	Sequencing samples	all clinical samples collected		
	PCH (average, n = 4)	Concentric hypertrophy (n = 12–16)	Eccentric hypertrophy (n = 11–19)	p value
LV structure and function				
LVEDD (mm)	45.5	**49.375 ± 9.6116**	**61.9474 ± 7.9055**	**0.0002**
LVESD (mm)	31	**36.375 ± 10.6701**	**51.5263 ± 8.8404**	**0.0001**
IVS (mm)	15.5	**14.325 ± 3.9408**	**8.3 ± 1.6496**	**<0.0001**
LVPWd (mm)	13	**12 ± 2.2804**	**8.6316 ± 1.1648**	**<0.0001**
LVEF (%)	57.5	**50.5625 ± 12.0884**	**35.2632 ± 8.6207**	**0.0001**
RV structure and function				
RV diameter (mm)	29.25	**31.1538 ± 4.2787**	**38.875 ± 8.123**	**0.0032**
TAPSE (mm)	19.25	20.3917 ± 6.1278	16.4786 ± 2.121	0.0547
TAPSV (cm/s)	12.475	16.0417 ± 5.979	15.0714 ± 3.1146	0.6195
Diastolic function				
Mitral E wave (cm/s)	3.1222	4.2258 ± 2.7983	3.3364 ± 2.2869	0.4159
Mitral annular e′(cm/s)	4.425	5.0083 ± 1.9365	5.2182 ± 1.4084	0.7711
E/e′ ratio	13	17.6333 ± 8.9467	15.5 ± 5.9564	0.4989
E/A ratio	0.6875	1.2875 ± 0.5633	1.4458 ± 0.9514	0.6248
TR velocity (m/s)	220	**217.5 ± 51.93**	**266.3571 ± 52.9639**	**0.0351**
heart failure marker				
BNP (pg/ml)	80.5	433.8 ± 461.3022 (n = 5)	950.9167 ± 727.2138 (n = 12)	0.1657
NT-proBNP (pg/ml)	/	3236.9231 ± 4410.0705 (n = 13)	9525.6667 ± 9690.4966 (n = 9)	0.0977

A: Mitral A wave, late diastolic mitral inflow velocity; BNP: B type natriuretic peptide; CON: control; e′: early diastolic mitral annular tissue velocity; E: Mitral E wave, early diastolic mitral inflow velocity; IVS: the thickness of the interventricular septum; LVEDD: left ventricular end-diastolic diameter; LVESD: left ventricular end-systolic diameter; LVPWd: left ventricular posterior wall dimensions; LVEF: left ventricular ejection fraction; NT-proBNP: N terminal pro B type natriuretic peptide; PCH: pathological cardiac hypertrophy; RV: right ventricular; TAPSE: tricuspid annular plane systolic excursion; TAPSV: tricuspid annular peak systolic velocity; TR, tricuspid regurgitation. Data are mean ± SD. $p < 0.05$ was regarded as significant. the $\chi 2$ test and unpaired t-test were used.

Overview Expression of tsRNAs in PCH and Control Groups

To identify the expression levels of tsRNAs in PCH and control groups, tsRNA-Seq was used for analysis. After quality filtering of the library data, we used Principal Component Analysis (PCA) for dimensionality reduction and visual presentation of large data sets, that is, tsRNAs that have the ANOVA p-value ≤ 0.05 on counts per million (CPM) value were used to show the distinguishable tsRNAs expression profiling among the samples (Figure 2A).

Differentially expressed tsRNAs analysis was performed with R package edgeR [20] and visualized with scatter plots. Fold change (>1.5) was used for screening differentially expressed tsRNAs. As shown in Figure 2B, compared with the control group, 1930 tsRNAs were up-regulated, 2255 tsRNAs were down-regulated and 649 tsRNAs were not observed to be differentially expressed.

The volcano plot is also a kind of scatter map. It combines the variation amplitude of tsRNAs expression level with statistical significance, which helps to quickly and intuitively identify tsRNAs with large variation amplitude and statistical significance. The horizontal axis is Log2 (fold change) of tsRNAs expression between the two groups, which is used to represent the multiple of difference. The vertical axis is -Log 10 (adjusted P-value) to show the significance of the difference. As shown in Figure 2C, 4 tsRNAs were observed to be significantly up-regulated, and 5 tsRNAs were observed to be

Preprints (www.preprints.org) | NOT PEER-REVIEWED | Posted: 24 April 2023 doi:10.20944/preprints202304.0855.v1

significantly down-regulated, suggesting that tsRNAs might have potential biological functions in PCH.

The result from hierarchical clustering shown by heatmap revealed the differences in tsRNAs expression profiles among samples. Compared with the control group, a total of 9 tsRNAs expressions in the PCH group were significantly dysregulated (Figure 2D).

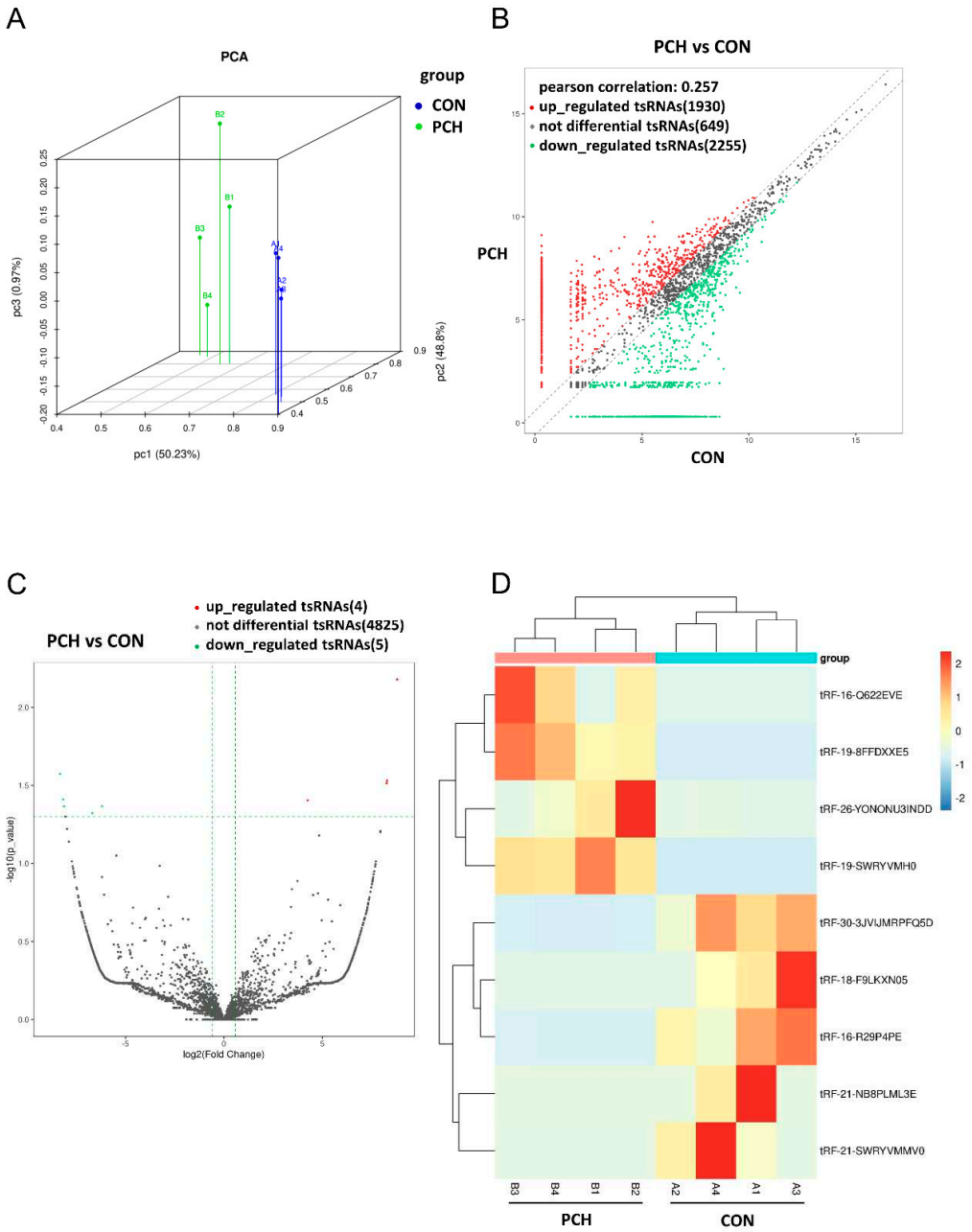

Figure 2. Expression profiles of tsRNAs sequencing data in the plasma of PCH patients and controls. (**A**) Primary component analysis. the X, Y, and Z axis represents the three main factors that affected the expression level of the samples. The colored point represents the corresponding samples, and the location of it shows the main character of the samples. Space distance represents the similarity of data size. (**B**) The scatter plot between two groups for tsRNAs. The CPM values of all tsRNAs are the plot. The values of the X and Y axes in the scatter plot are the averaged CPM values of each group (log2 scaled). tsRNAs above the top line (red dots, up-regulation) or below the bottom line (green dots, down-regulation) indicate more than a 1.5-fold change between the two compared groups. Gray dots indicate non-differentially expressed tsRNAs. (**C**) The volcano plot of tsRNAs. The values of the X

Preprints (www.preprints.org) | NOT PEER-REVIEWED | Posted: 24 April 2023 doi:10.20944/preprints202304.0855.v1

and Y axes in the volcano plot are log2 transformed fold change and -log10 transformed p-values between the two groups, respectively. Red/Green circles indicate statistically significant differentially expressed tsRNAs with fold change no less than 1.5 and p-value ≤ 0.05 (Red: up-regulated; Green: down-regulated). Gray circles indicate non-differentially expressed tsRNAs, with FC and/or q-value not meeting the cutoff thresholds. (**D**) Heatmap showing the hierarchical clustering of differentially expressed tsRNAs. CON: control; PCH: pathological cardiac hypertrophy.

Validation for the Differentially Dysregulated Expression of tsRNAs

Real-time qPCR was performed to validate the down-regulated 5 tsRNAs. Among them, tRF-18-F9LKXN05 could not be detected due to low expression levels in plasma. As the results showed in Figure 3A, the expressions of tRF-30-3JVIJMRPFQ5D, tRF-16-R29P4PE, tRF-21-NB8PLML3E, and tRF-21-SWRYVMMV0 were significantly downregulated ($p < 0.05$ or $p < 0.01$). With the progression of PCH, the expression levels of the four down-regulated tsRNAs all seemed to increase in the eccentric hypertrophy stage compared with the concentric hypertrophy stage, but the differences were not significant (Figure 3B). Especially, they were decreased in the Ang II-stimulated H9c2 cells (Figure 4C) consistent with the changes in plasma.

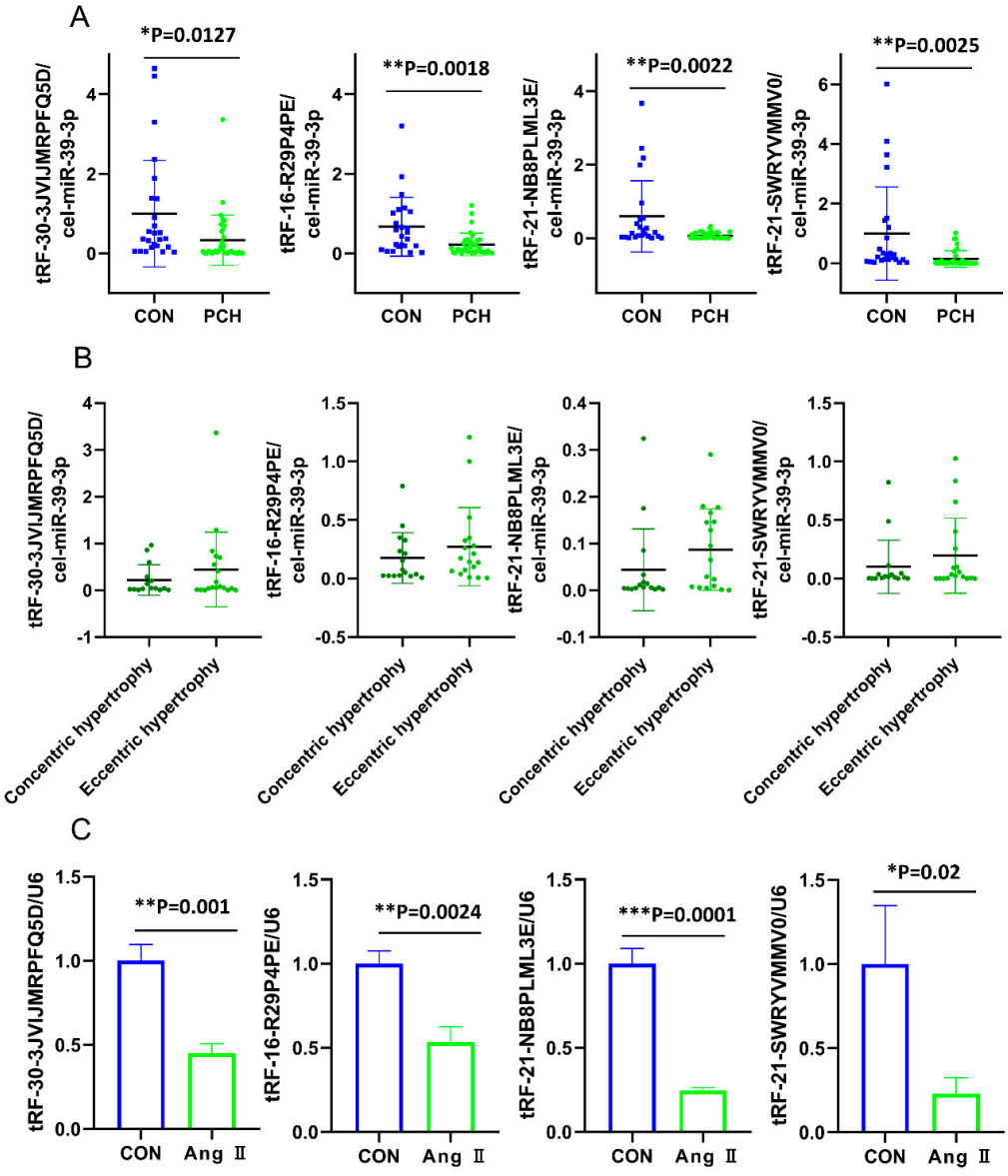

Figure 3. Validation of the relative expression level of down-regulated tsRNAs by real-time qPCR. The plasma of 35 PCH patients and 25 controls were used for validation. The statistical significance

 doi:10.20944/preprints202304.0855.v1

between PCH and controls was calculated by the Student t-test. Data were expressed as the means ± SD. (**A**) The relative expression of the 4 down-regulated tsRNAs between PCH and CON. (**B**) The relative expression of the 4 down-regulated tsRNAs between concentric hypertrophy and eccentric hypertrophy. $p < 0.05$ was considered statistically significant. (**C**) The relative expression of 4 down-regulated tsRNAs between the control H9c2 group and the Ang II-stimulated H9c2 group ($n = 3$). $p < 0.05$ was considered statistically significant. * $p < 0.05$, ** $p < 0.01$. CON: control; PCH: pathological cardiac hypertrophy.

ROC Analysis of Validated tsRNAs in PCH Patients

According to the relative expression levels of these 4 proven tsRNAs (tRF-30-3JVIJMRPFQ5D, tRF-16-R29P4PE, tRF-21-NB8PLML3E and tRF-21-SWRYVMMV0) in plasma of PCH patients and healthy controls, ROC curves were generated to analyze the diagnostic potential of differentially expressed tsRNAs (Figure 4A). The values of area under the ROC curve (AUC) of these 4 tsRNAs were 0.7423, 0.7497, 0.7726, and 0.836 respectively. According to the principle of ROC curve, a larger AUC generally means a better diagnostic potential. In addition, considering the p-value, sensitivity and specificity, tRF-21-SWRYVMMV0 and tRF-21-NB8PLML3E were the preferred biomarkers for the diagnosis of PCH.

Further, to analyze the early-stage screening potential of differentially expressed tsRNAs in PCH, ROC curves were generated for the four tsRNAs in concentric hypertrophy and eccentric hypertrophy, respectively (Figure 4B–E), and the values of AUC, p value, sensitivity and specificity were analyzed (Table S3). The ROC curve results showed that the early-stage screening potential of the four tsRNAs was better than that of the late stage, and tRF-21-SWRYVMMV0 and tRF-21-NB8PLML3E showed good diagnostic potential in the entire course of PCH.

Correlations of Validated tsRNAs Expression with Disease Phenotypes in PCH Patients

The disease phenotypes of PCH compared with the corresponding expression level of validated tsRNAs are listed in Table S4. The main pathological indicators of PCH are IVS, LVPWd, LVEDD and LVEF. The four validated tsRNAs were all significantly negatively correlated with LVPWd (Figure 5A), and more so in eccentric hypertrophy (Figure 5B,C). In addition, tRF-21-NB8PLML3E was also significantly negatively correlated with LVEF (Table S4).

Preprints (www.preprints.org) | NOT PEER-REVIEWED | Posted: 24 April 2023 doi:10.20944/preprints202304.0855.v1

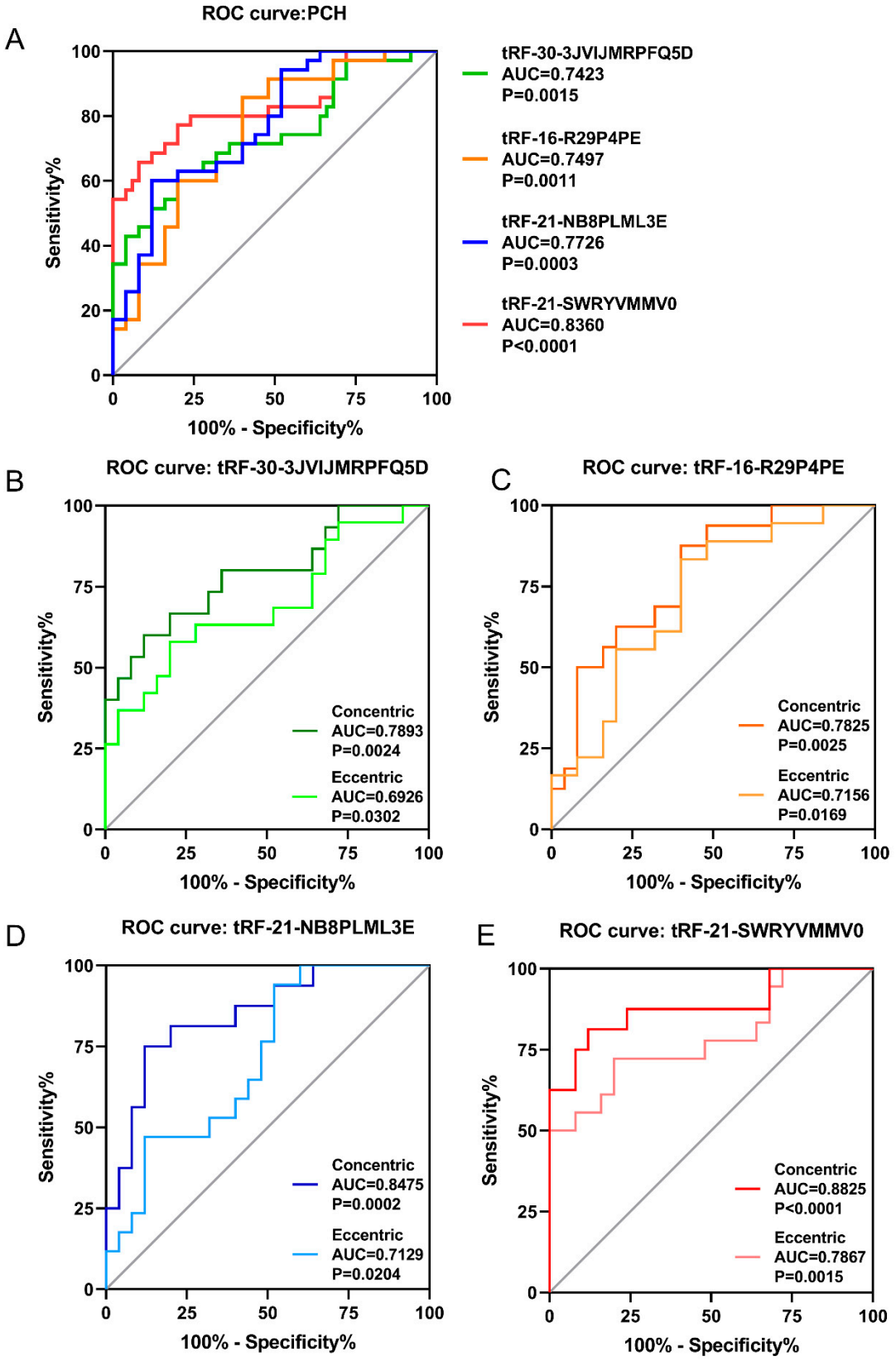

Figure 4. ROC curve analysis to evaluate the diagnostic value of validated tsRNAs. (**A**) ROC curves of the 4 down-regulated tsRNAs in PCH (n = 35). (**B**–**E**) ROC curves of the 4 tsRNAs in concentric hypertrophy (n = 16) and eccentric hypertrophy (n = 19), respectively. AUC = area under curve; PCH: pathological cardiac hypertrophy; ROC = receiver operating characteristic.

Preprints (www.preprints.org) | NOT PEER-REVIEWED | Posted: 24 April 2023 doi:10.20944/preprints202304.0855.v1

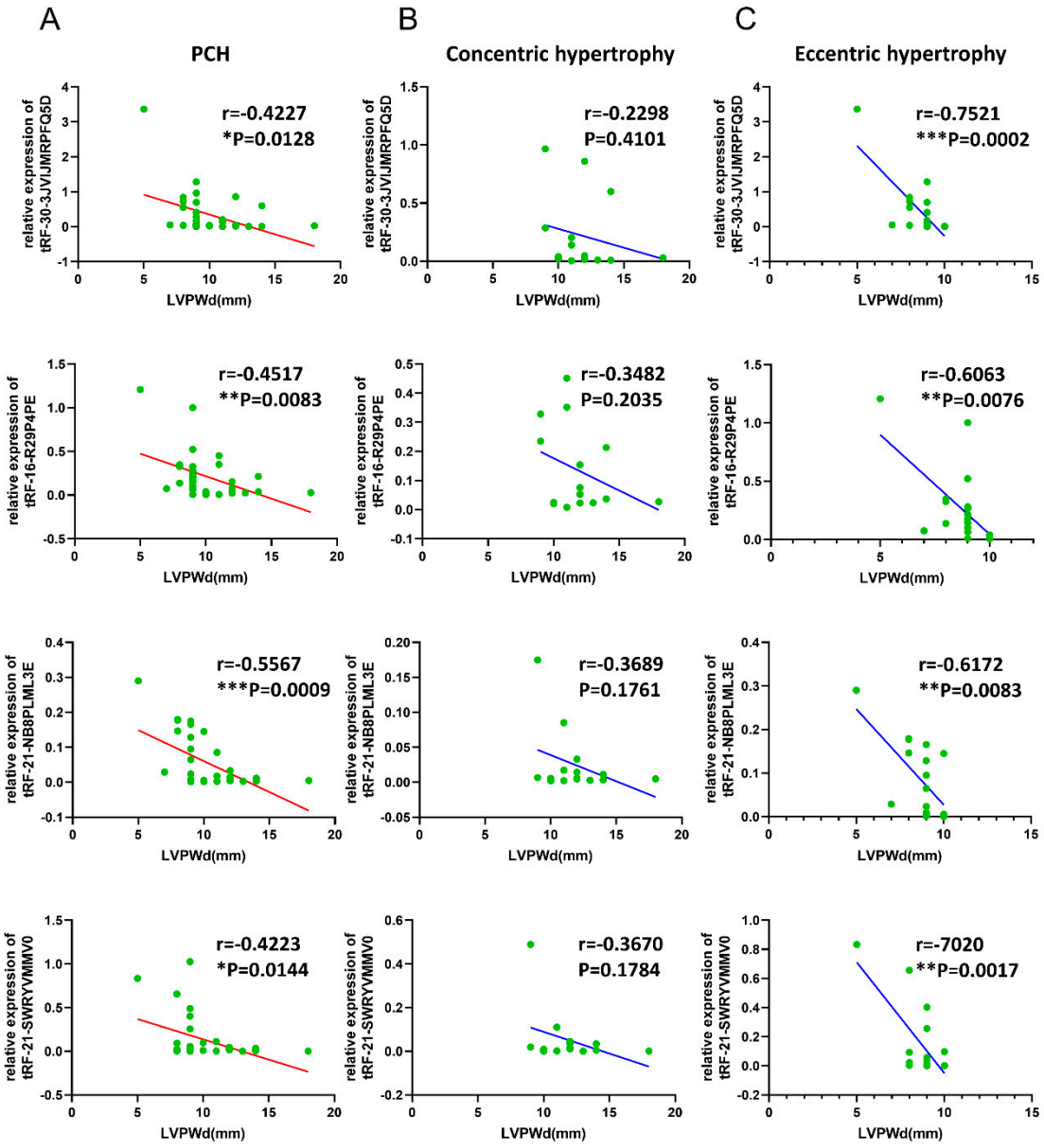

Figure 5. Correlations of validated tsRNAs expression with LVPWd in PCH patients. Spearman's analysis was applied to test the correlation of validated tsRNAs expression with disease activity. (**A**) Correlations of the 4 down-regulated tsRNAs expression with LVPWd in PCH (n = 35); (**B**): Correlations of the four down-regulated tsRNAs expressions with LVPWd in concentric hypertrophy (n = 16); (**C**): Correlations of the four down-regulated tsRNAs expressions with LVPWd in eccentric hypertrophy (n = 19). $p < 0.05$ was considered statistically significant. * $p < 0.05$, ** $p < 0.01$. LVPWd: left ventricular posterior wall dimensions. PCH: pathological cardiac hypertrophy.

Effects of tRF-21-NB8PLML3E in Ang II-Stimulated H9c2 Cells

The results showed that the tRF-21-NB8PLML3E expression in the mimic or inhibitor transfected group was significantly increased or decreased as compared with the control group (Figure 6A, $p < 0.01$), indicating an effective transfection. As shown in Figure 6B,C, the levels of ANP and BNP were significantly decreased in tRF-21-NB8PLML3E mimic transfected cells. The immunofluorescence results showed that tRF-21-NB8PLML3E mimic treatment could alleviate Ang II-induced cardiomyocyte hypertrophy.

Preprints (www.preprints.org) | NOT PEER-REVIEWED | Posted: 24 April 2023 doi:10.20944/preprints202304.0855.v1

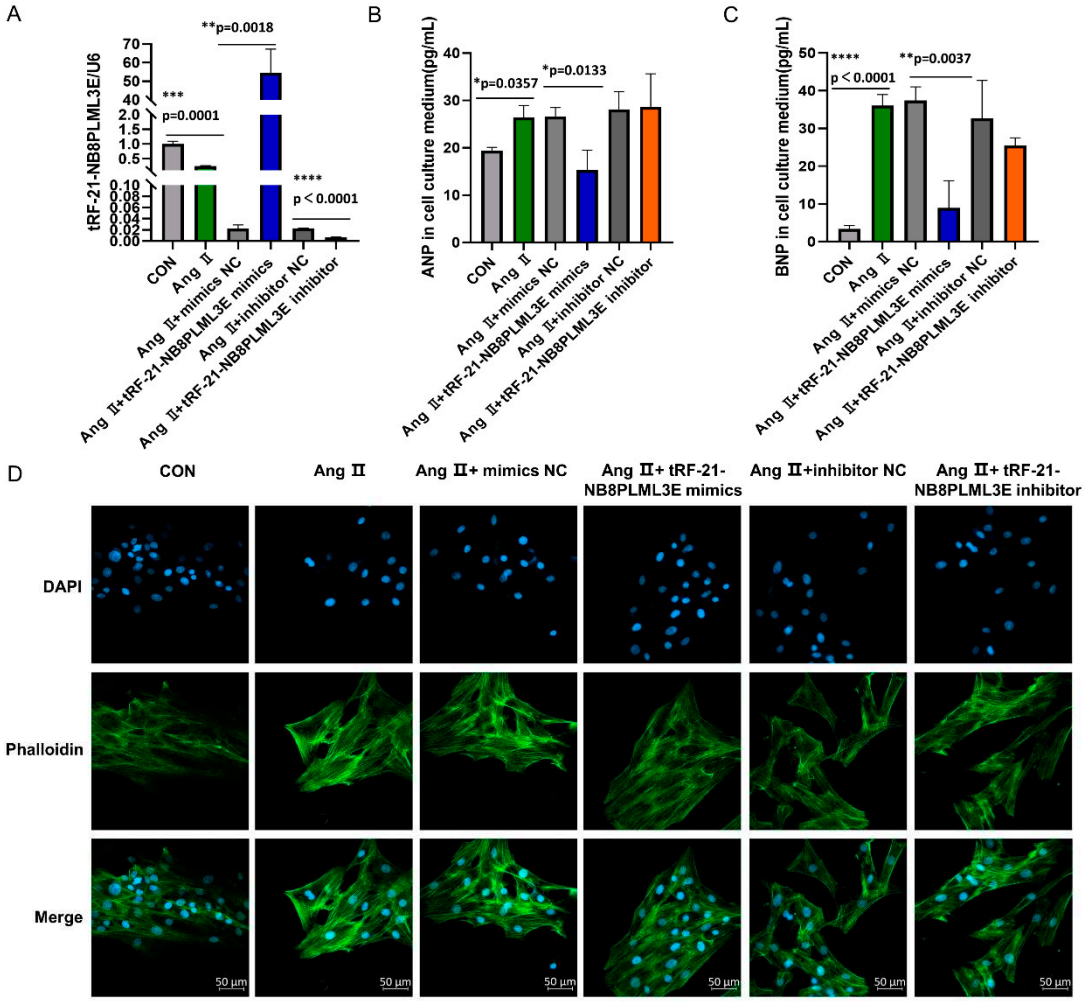

Figure 6. Intracellular tRF-21-NB8PLML3E, ANP, and BNP expressions as well as Cytoskeleton staining in tRF-21-NB8PLML3E mimic/inhibitor-transfected Ang II-stimulated H9c2 cells. (**A**) tRF-21-NB8PLML3E expression. (**B**) ANP expression. (**C**) BNP expression. (**D**) immunofluorescence photo (phalloidin stained green, scale bar: 50 μm). Data are expressed as the mean ± SD, with n = 3per group. $p < 0.05$ was considered statistically significant. * $p < 0.05$, ** $p < 0.01$, *** $p < 0.001$, **** $p < 0.0001$. CON: control; NC: Negative control.

Biological Information Function Analysis of tsRNAs with Diagnostic Potential

Figure 7A showed sequence information for tRF-21-NB8PLML3E with diagnostic potential. Studies have shown that many tsRNA can perform roles similar to miRNAs, including interacting with Argonaute, producing in a dicer-dependent manner, and can participate in translation silencing [20,21]. So, to further explore the potential roles of tRF-21-NB8PLML3E in PCH, we identified the associated target genes with miRNA target prediction algorithm TargetScan and miRanda algorithms. The number of target genes was 56 for tRF-21-NB8PLML3E (Figure 7B).

To predict the potential biological functions of these target genes, we evaluated them using GO and KEGG enrichment analyses. In the biological process of GO analysis, the top ten enriched terms that may be related to cardiovascular disease are displayed in Figure 7C, indicating that the potential target genes of tRF-21-NB8PLML3E are mainly responsible for the biogenesis process of the ribosome, Golgi.

Significant pathways for each tsRNA were ranked by adjusted p-value according to KEGG pathway analysis. The signaling pathway of tRF-21-NB8PLML3E is mainly enriched in alpha-Linolenic acid metabolism, Sphingolipid metabolism, Mitophagy, Adherens junction, Fc gamma R-mediated phagocytosis and Glycerophospholipid metabolism (Figure 7D).

Preprints (www.preprints.org) | NOT PEER-REVIEWED | Posted: 24 April 2023 doi:10.20944/preprints202304.0855.v1

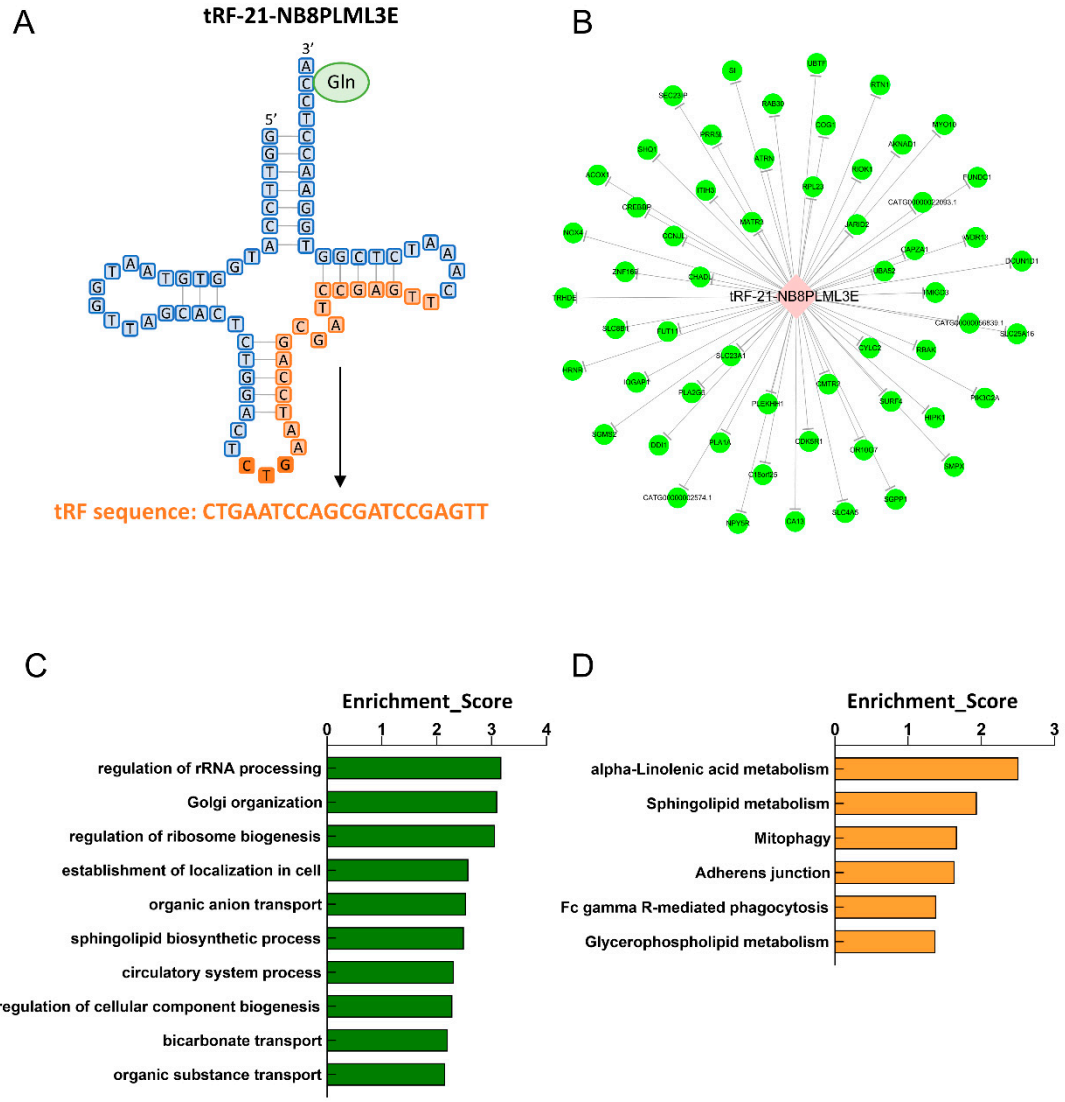

Figure 7. Integrated analysis of validated tsRNAs. (**A**) Sequence information for tRF-21-NB8PLML3E. (**B**) The potentially altered target mRNAs of tRF-21-NB8PLML3E. (**C**) The Gene Ontology (GO) enrichment analyses of tRF-21-NB8PLML3E. (**D**) KEGG pathway analysis for tRF-21-NB8PLML3E gathering genes. The vertical axis shows the annotated functions of the target genes. The horizontal axis shows the enrichment score (-log10 transformed p-value), respectively. Only the most significantly enriched clusters are included.

Discussion

As the most ancient small RNAs in all domains of life, tsRNAs have good sequence conservation [22]. In addition, tsRNAs are present in all types of body fluids [23] and are dynamically regulated by pathophysiological conditions [24]. Based on these properties, tsRNAs might be excellent candidates as liquid biopsy biomarkers.

Due to the sequence conservation of tsRNAs, they play a variety of functions in fundamental biological processes, including gene silencing, ribosomal biogenesis, retro transposition, and epigenetic inheritance [22]. These functions make it possible for tsRNAs to regulate gene expression at the transcriptional and post-transcriptional levels, thus playing a key regulatory role in multiple pathological events [25].

In recent years, the application of tsRNAs in cardiovascular diseases has received more and more attention. Studies have shown that 5′-tiRNA-Cys-GCA could inhibit the aortic dissection via

the signal transducer and activator of the transcription 4 signaling pathway [26]. The synthetic tRF (GlnCTG) could negatively regulate the expression of FAS cell surface death receptors to elevate the proliferation and migration of vascular smooth muscle cells [27]. tiRNA-Gln-TTG-001 might be considered as a novel biomarker and therapeutic target for myocarditis [28]. Thus, these findings provide some evidence for the association between aberrant tsRNAs expression and cardiovascular system dysfunction.

Given the pleiotropic roles of tsRNAs in the cardiovascular system, the purpose of this study was to investigate whether tsRNAs are involved in PCH. We first detected the expression profile of tsRNAs in the plasma of PCH patients and healthy volunteers by RNA sequencing. The results showed that there were 9 tsRNAs were significantly differentially expressed. Then, we performed real-time qPCR to further validate the significantly down-regulated expressed tsRNAs in line with sequencing data. As the results showed, the expressions of tRF-30-3JVIJMRPFQ5D, tRF-16-R29P4PE, tRF-21-NB8PLML3E, and tRF-21-SWRYVMMV0 were significantly downregulated. However, with the progression of PCH, the expression levels of the four tsRNAs seemed to rebound slightly, which deserves further investigation. Among the 4 tsRNAs, ROC curve analysis indicated that tRF-21-NB8PLML3E might serve as biomarkers for early screening of PCH. Especially, in the present study, we observed that in Ang II-stimulated H9c2 cells, the tRF-21-NB8PLML3E expression was decreased, and the addition of tRF-21-NB8PLML3E mimic could simultaneously reverse the tRF-21-NB8PLML3E expression and inhibit ANP and BNP expressions as well as attenuate cardiomyocyte hypertrophy. From these experimental and literature data, we thought that tRF-21-NB8PLML3E might improve Ang II-induced H9c2 cells hypertrophy, and the specific mechanisms of tRF-21-NB8PLML3E on PCH need to be investigated.

Interestingly, through correlation analysis with clinical phenotypes, it was found that the 4 tsRNAs showed negative correlations with LVPWd, and the correlation gradually increased with the progression of PCH. This result suggests that tsRNAs are more and more closely involved in the development of PCH, which also indicates that tsRNAs not only have the potential of biomarkers in the early screening and diagnosis of PCH but also the potential in treatment is worthy of attention. Therefore, it is necessary for us to further explore the roles in pathogenesis.

To further confirm the roles of tRF-21-NB8PLML3E in PCH, target genes were predicted by miRnada algorithms and TargetScan, and GO analysis and KEGG pathway analysis were performed on the target genes. For tRF-21-NB8PLML3E, we found that its target genes may be closely related to the biogenesis process of the ribosome by GO analysis. Supporting the result of this analysis, recent evidence has shown that, stress-induced tsRNAs can flexibly promote or inhibit protein translation, which might be closely related to where and how they interact with the ribosome. [22]. According to KEGG pathway analysis, the 6 signaling pathways enriched by tRF-21-NB8PLML3E are mainly related to metabolism. It is generally accepted that the disorder of the cardiac metabolic process is the common pathogenesis factor of PCH [29,30]. It has been shown that impaired adaptation of energy metabolism can exacerbate pathological hypertrophy and increase cardiomyocyte death [31]. Impairment of fatty acid and pyruvate metabolism causes mitochondrial dysfunction, oxidative stress, and contractile dysfunction [32]. Dysregulation of fatty acid or carbohydrate metabolism directly induces cardiac hypertrophy and/or functional decline in genetically engineered mice by regulating pathological signaling mechanisms [33–35]. Therefore, we deduced that tRF-21-NB8PLML3E might exert the regulatory effects of PCH, and the roles might partially associate with the regulation of metabolic processes in the dysfunctional heart.

Study Limitations

There are certain limitations to our study. First, the insufficient number of subjects might correspondingly lead to some data bias. Second, in addition to playing roles similar to miRNAs, tsRNAs also have other mechanisms of action. However, since there is no independent target prediction algorithm for tsRNA at present, we chose miRNA target prediction algorithm for preliminary functional analysis to speculate the possible role of tsRNAs in PCH without experimental verification.

Conclusion

Our study provided the expression profiles of tsRNAs in plasmas of PCH patients for the first time. Validation results by integrated next-generation sequencing analysis and qPCR demonstrated that tsRNAs in plasma are valuable for the diagnosis of PCH. Furthermore, tRF-21-NB8PLML3E might be the preferred diagnostic biomarkers for PCH. Nonetheless, further studies are required to explore the molecular mechanisms of tRF-21-NB8PLML3E in PCH development.

Author Contributions: J Xu and B Qian analyzed the data and wrote the original draft article. J Xu, B Qian, Y Huang, F Wang, Q Zhang, and Y Li collected samples. F Wang, Y Huang, X Yan, and P Li performed qPCR. Y Li and K Sun designed the experiment and revised the article. J Xu and B Qian contributed equally to this work. Y Li and K Sun are co-corresponding authors of this work. All authors read and approved the final manuscript.

Funding: This research was supported by a grant from the Scientific Research Project of Gusu College, Nanjing Medical University (grant number GSKY20210202 to K Sun), Fund of Nanjing Medical University Science and Technology Development (grant number NMUB20210271 to J Xu), Applied Foundational Research of Medical and Health Care of Suzhou City (grant number SKJY2021120 to F Wang), Scientific research project of Jiangsu Provincial Health Commission (grant number M2021099 to F Wang), Youth Project of Jiangsu Basic Research Program (Natural Science Foundation) (grant number BK20190189 to X Yan) and Science and Technology Development Fund of Suzhou for Youth (grant number KJXW2021039 to P Li and KJXW2020038 to F Wang).

Ethical Conduct of Research: The study was approved and supervised by the Ethics Committees of Affiliated Suzhou Hospital of Nanjing Medical University, Gusu School (K-2021-GSKY20210202). Informed consent has been obtained from the participants involved.

Data Availability Statement: The data that support the findings of this study are available from the corresponding author upon reasonable request.

Acknowledgments: The authors thank the patients and volunteers that participated in this study.

Conflict of Interest: The Authors declare that there is no conflict of interest.

References

1. Frey, N.; Olson, E.N. Cardiac hypertrophy: The good, the bad, and the ugly. *Annu. Rev. Physiol.* **2003**, *65*, 45–79.
2. Schirone, L.; Forte, M.; Palmerio, S.; Yee, D.; Nocella, C.; Angelini, F.; et al. A review of the molecular mechanisms underlying the development and progression of cardiac remodeling. *Oxid. Med. Cell. Longev.* **2017**, *2017*, 3920195.
3. Nakamura, M.; Sadoshima, J. Mechanisms of physiological and pathological cardiac hypertrophy. *Nat. Rev. Cardiol.* **2018**, *15*, 387–407.
4. Lu, P.; Ding, F.; Xiang, Y.K.; Hao, L.; Zhao, M. Noncoding RNAs in cardiac hypertrophy and heart failure. *Cells* **2022**, *11*.
5. Lin, X.; Zhang, L.; Zhang, W.; Lei, X.; Lu, Q.; Ma, A. Circular RNA circ_0001006 aggravates cardiac hypertrophy via miR-214-3p/PAK6 axis. *Aging (Albany NY)* **2022**, *14*, 2210–2220.
6. Jusic, A.; Thomas, P.B.; Wettinger, S.B.; Dogan, S.; Farrugia, R.; Gaetano, C.; et al. Noncoding RNAs in age-related cardiovascular diseases. *Ageing Res. Rev.* **2022**, *77*, 101610.
7. Kwon NH, Lee JY, Kim S. Role of tRNAs in breast cancer regulation. Adv Exp Med Biol. **2021**, *1187*, 121–145.
8. Shen, Y.; Yu, X.; Zhu, L.; Li, T.; Yan, Z.; Guo, J. Transfer RNA-derived fragments and tRNA halves: Biogenesis, biological functions and their roles in diseases. *J. Mol. Med. (Berl.)* **2018**, *96*, 1167–1176.
9. Lee, Y.S.; Shibata, Y.; Malhotra, A.; Dutta, A. A novel class of small RNAs: tRNA-derived RNA fragments (tRFs). *Genes Dev.* **2009**, *23*, 2639–2649.
10. Chen, H.; Xu, Z.; Liu, D. Small non-coding RNA and colorectal cancer. *J. Cell. Mol. Med.* **2019**, *23*, 3050–3057.
11. Li, S.; Xu, Z.; Sheng, J. tRNA-derived small RNA: A novel regulatory small non-coding RNA. *Genes* **2018**, *9*.
12. Kumar, P.; Kuscu, C.; Dutta, A. Biogenesis and function of transfer RNA-related fragments (tRFs). *Trends Biochem. Sci.* **2016**, *41*, 679–689.
13. Kim, H.K.; Fuchs, G.; Wang, S.; Wei, W.; Zhang, Y.; Park, H.; et al. A transfer-RNA-derived small RNA regulates ribosome biogenesis. *Nature* **2017**, *552*, 57–62.
14. Zheng, L.L.; Xu, W.L.; Liu, S.; Sun, W.J.; Li, J.H.; Wu, J.; et al. tRF2Cancer: A web server to detect tRNA-derived small RNA fragments (tRFs) and their expression in multiple cancers. *Nucleic Acids Res.* **2016**, *44*, W185–W193.

15. Xiao, L.; Wang, J.; Ju, S.; Cui, M.; Jing, R. Disorders and roles of tsRNA, snoRNA, snRNA and piRNA in cancer. *J. Med. Genet.* **2022**, *59*, 623–631.
16. Peng, G.; Sun, Q.; Chen, Y.; Wu, X.; Guo, Y.; Ji, H.; et al. A comprehensive overview of ovarian small non-coding RNAs in the late overwintering and breeding periods of Onychostoma macrolepis. *Comp. Biochem. Physiol. Part D Genom. Proteom.* **2022**, *42*, 100967.
17. Peng, R.; Santos, H.J.; Nozaki, T. Transfer RNA-derived small RNAs in the pathogenesis of parasitic protozoa. *Genes* **2022**, *13*.
18. Guzzi, N.; Ciesla, M.; Ngoc, P.C.T.; Lang, S.; Arora, S.; Dimitriou, M.; et al. Pseudouridylation of tRNA-derived fragments steers translational control in stem cells. *Cell* **2018**, *173*, 1204–1216 e26.
19. Zhong, F.; Hu, Z.; Jiang, K.; Lei, B.; Wu, Z.; Yuan, G.; et al. Complement C3 activation regulates the production of tRNA-derived fragments Gly-tRFs and promotes alcohol-induced liver injury and steatosis. *Cell Res.* **2019**, *29*, 548–561.
20. Meta-analysis of tRNA derived RNA fragments reveals that they are evolutionarily conserved and associate with AGO proteins to recognize specific RNA targets. *BMC Biol.* **2014**, *12*, 78.
21. Schorn, A.J.; Gutbrod, M.J.; LeBlanc, C.; Martienssen, R. LTR-retrotransposon control by tRNA-derived small RNAs. *Cell* **2017**, *170*, 61–71.e11.
22. Chen, Q.; Zhang, X.; Shi, J.; Yan, M.; Zhou, T. Origins and evolving functionalities of tRNA-derived small RNAs. *Trends Biochem. Sci.* **2021**, *46*, 790–804.
23. Godoy, P.M.; Bhakta, N.R.; Barczak, A.J.; Cakmak, H.; Fisher, S.; MacKenzie, T.C.; et al. Large differences in small RNA composition between human biofluids. *Cell Rep.* **2018**, *25*, 1346–1358.
24. Zhang, Y.; Zhang, Y.; Shi, J.; Zhang, H.; Cao, Z.; Gao, X.; et al. Identification and characterization of an ancient class of small RNAs enriched in serum associating with active infection. *J. Mol. Cell Biol.* **2014**, *6*, 172–174.
25. Zhu, C.; Sun, B.; Nie, A.; Zhou, Z. The tRNA-associated dysregulation in immune responses and immune diseases. *Acta Physiol. (Oxf.)* **2020**, *228*, e13391.
26. Zong, T.; Yang, Y.; Lin, X.; Jiang, S.; Zhao, H.; Liu, M.; et al. 5′-tiRNA-Cys-GCA regulates VSMC proliferation and phenotypic transition by targeting STAT4 in aortic dissection. *Mol. Ther. Nucleic Acids* **2021**, *26*, 295–306.
27. Zhu, X.L.; Li, T.; Cao, Y.; Yao, Q.P.; Liu, X.; Li, Y.; et al. tRNA-derived fragments tRF(GlnCTG) induced by arterial injury promote vascular smooth muscle cell proliferation. *Mol. Ther. Nucleic Acids* **2021**, *23*, 603–613.
28. Wang, J.; Han, B.; Yi, Y.; Wang, Y.; Zhang, L.; Jia, H.; et al. Expression profiles and functional analysis of plasma tRNA-derived small RNAs in children with fulminant myocarditis. *Epigenomics* **2021**, *13*, 1057–1075.
29. Osaka, N.; Mori, Y.; Terasaki, M.; Hiromura, M.; Saito, T.; Yashima, H.; et al. Luseogliflozin inhibits high glucose-induced TGF-beta2 expression in mouse cardiomyocytes by suppressing NHE-1 activity. *J. Int. Med. Res.* **2022**, *50*, 3000605221097490.
30. Sun, W.; Zhou, Y.; Xue, H.; Hou, H.; He, G.; Yang, Q. Endoplasmic reticulum stress mediates homocysteine-induced hypertrophy of cardiac cells through activation of cyclic nucleotide phosphodiesterase 1C. *Acta Biochim. Biophys. Sin. (Shanghai)* **2022**, *54*, 388–399.
31. Doenst, T.; Nguyen, T.D.; Abel, E.D. Cardiac metabolism in heart failure: Implications beyond ATP production. *Circ. Res.* **2013**, *113*, 709–724.
32. Boudina, S.; Bugger, H.; Sena, S.; O'Neill, B.T.; Zaha, V.G.; Ilkun, O.; et al. Contribution of impaired myocardial insulin signaling to mitochondrial dysfunction and oxidative stress in the heart. *Circulation* **2009**, *119*, 1272–1283.
33. Yagyu, H.; Chen, G.; Yokoyama, M.; Hirata, K.; Augustus, A.; Kako, Y.; et al. Lipoprotein lipase (LpL) on the surface of cardiomyocytes increases lipid uptake and produces a cardiomyopathy. *J. Clin. Investig.* **2003**, *111*, 419–426.
34. Chiu, H.C.; Kovacs, A.; Blanton, R.M.; Han, X.; Courtois, M.; Weinheimer, C.J.; et al. Transgenic expression of fatty acid transport protein 1 in the heart causes lipotoxic cardiomyopathy. *Circ. Res.* **2005**, *96*, 225–233.
35. Cheng, L.; Ding, G.; Qin, Q.; Huang, Y.; Lewis, W.; He, N.; et al. Cardiomyocyte-restricted peroxisome proliferator-activated receptor-delta deletion perturbs myocardial fatty acid oxidation and leads to cardiomyopathy. *Nat. Med.* **2004**, *10*, 1245–1250.